ATG8 delipidation is dispensable for plant autophagy

Sanjana Holla[1], Yong Zou[1], Igor Sabljic[1], Jonas A Ohlsson[1, ¶], Jia Xuan Leong[2,3, ¶], Florentine Ballhaus[1], Melanie Krebs[2], Karin Schumacher[2], Peter V Bozhkov[1] and Elena A Minina [1,2, ¶]

[1]Department of Molecular Sciences, Uppsala BioCenter, Swedish University of Agricultural Sciences and Linnean Center for Plant Biology, Uppsala, SE-750 07, Sweden

[2]Centre for Organismal Studies (COS), Heidelberg University. Im Neuenheimer Feld 230. 69120 Heidelberg, Germany

[3]Center for Plant Molecular Biology (ZMBP), University of Tübingen, Auf der Morgenstelle 32. D-72076 Tübingen, Germany

[¶]Corresponding authors:

Alyona Minina: alena.minina@slu.se

Abstract

Autophagy is a catabolic pathway conserved across eukaryotes. It plays a vital role in diverse stress responses by dismantling and recycling unnecessary or dysfunctional cellular parts and is orchestrated by the **a**u**t**opha**g**y related ATG proteins conserved among all eukaryotes[1,2]. An astounding conservation of autophagic machinery across eukaryotes highlights the fundamental role it plays in the cell's homeostasis. In this study we discovered that ATG4-dependent delipidation of ATG8, previously considered as critical step in autophagy mechanism of all eukaryotes, is dispensable in *Arabidopsis thaliana*. Moreover, using ATG4-deficient background as a model system we uncovered specific function of two Arabidopsis ATG8 orthologs in autophagosome formation. Finally, we demonstrated that ATG8 delipidation is critical for autophagy in evolutionary distant from Arabidopsis species, unicellular green algae *Chlamydomonas reinhardtii*.

These findings provide a new insight on plant-specific aspect of autophagy, highlight important differences between higher and lower plants and she new light on the reasons behind ATG8 gene family expansion.

Introduction

Autophagy plays a vital role in sustaining functionality of cellular constituents and helping to overcome nutrient scarcity. It sequesters superfluous or dysfunctional cytoplasmic cargo into double membrane-vesicles, autophagosomes, and delivers them for degradation to the lytic compartment. This process is orchestrated by the ATG proteins conserved among all eukaryotes[1,2].

Intriguingly, the evolution of autophagy repurposed certain constituents from the more ancient catabolic pathway, UPS[3]: ubiquitin-like ATG8 protein undergoes a series of post-translational modifications that closely resemble the proteolytic processing, of ubiquitin and its activation, conjugation, and ligation executed by E1, E2 and E3 enzymes[1,4,5]. Akin to ubiquitin[6], ATG8 undergoes the removal of its C-terminal peptide by a dedicated protease (ATG4), exposing the essential C-terminal glycine residue for subsequent modifications[5]. The exposed Gly of ATG8 is subsequently activated by the E1-like enzyme ATG7, and further transferred to the E2-like enzyme ATG3. Lastly, a protein complex with the E3-like activity (ATG12–ATG5-ATG16) ligates the C-terminal Gly of ATG8 with phosphatidylethanolamine (PE) [5] anchoring it in the forming autophagosomal membranes (Fig.1A)[7]. The ATG8-PE decorates inner and outer membranes of the forming autophagosome and plays crucial roles in the cargo sequestration and the formation, closure and fusion of autophagosomes[8].

Crucially, at the later stages of formation, ATG4 releases ATG8 from the outer membrane of autophagosomes by cutting the amide bond between it and PE [9–11]. This enables recycling of ATG8 for formation of new autophagosomes, akin to how deubiquitinating enzymes recycle ubiquitin back into the cellular pool[6]. In yeast and animal autophagy, the delipidation of ATG8 is thought to facilitate the detachment of other core ATG proteins from mature autophagosomes and signaling their readiness for docking and fusion with the lytic compartment.[4,12,13]

Yeasts and unicellular lower plants have single copies of core ATG genes in their genomes, making them excellent models to study conserved autophagy features. In more complex organisms, ATG gene families have expanded and obtained diversified functions, offering insights into intricate autophagy features. For example, Arabidopsis genome contains two genes for ATG4 (*ATG4A* and *B*) and 9 genes coding for ATG8 isoforms, named ATG8A to ATG8I [14]. Notably, certain plant ATG8 orthologs lack C-terminal extensions, enabling direct lipidation without ATG4 processing[14]. However, little is known about specific functions of plant these ATG8 proteins[15,16].

Current evidence indicates that ATG8 delipidation occurs in all eukaryotes. In animal cells this process is critical for autophagosomal docking and fusion with lysosomes[4,17]. Intriguingly, abrogation of ATG8 delipidation in yeast impairs autophagic activity at a different step of the pathway –

elongation of the autophagosomal membranes[12,18]. These discrepancies point out important differences in maturation of yeast and animal autophagosomes.

ATG8 delipidation was suggested to be essential for plant autophagy as well, by a study focused on ATG4-deficient Arabidopsis plants that expressedd ATHG8H and I isoforms, lacking the C-terminal peptides thereby necessitating ATG4 activity solely for delipidation. The lack of detectable autophagic activity in these plants was explained by impairment of ATG8 delipidation[11].

In this study we demonstrate that expression of the artificially truncated ATG8E isoform restored autophagic activity in the ATG4-deficient Arabidopsis, thereby showing that previously reported phenotype was ATG8 isoform-specific and plant autophagosomes can mature without ATG8 delipidation. Furthermore, we investigated whether the same phenomenon could be observed in lower plants, by testing it in the unicellular algae *Chlamydomonas reinhardtii*. Autophagic activity in this model organism was strongly dependent on delipidation of the sole endogenous ATG8.

Results

ATG8ΔC labels autophagic bodies in the vacuoles of the ATG4-deficeint cells.

We generated stable Arabidopsis lines expressing in the wild-type (WT) or ATG4-deficient (*atg4a/b*) backgrounds three variants of EosFP-tagged ATG8E isoform: full length ATG8, G/A mutant not applicable for lipidation and ATG8ΔC, truncated protein lacking the C-terminal peptide and thereby having the critical for lipidation glycine residue readily exposed (**Fig.1B**). The seedlings of these lines were treated with autophagy-inducing compound AZD8055 and vacuolar pH-increasing compound Concanamycin A (ConA), which prevents degradation of the autophagosomes delivered to the plant vacuoles[19].

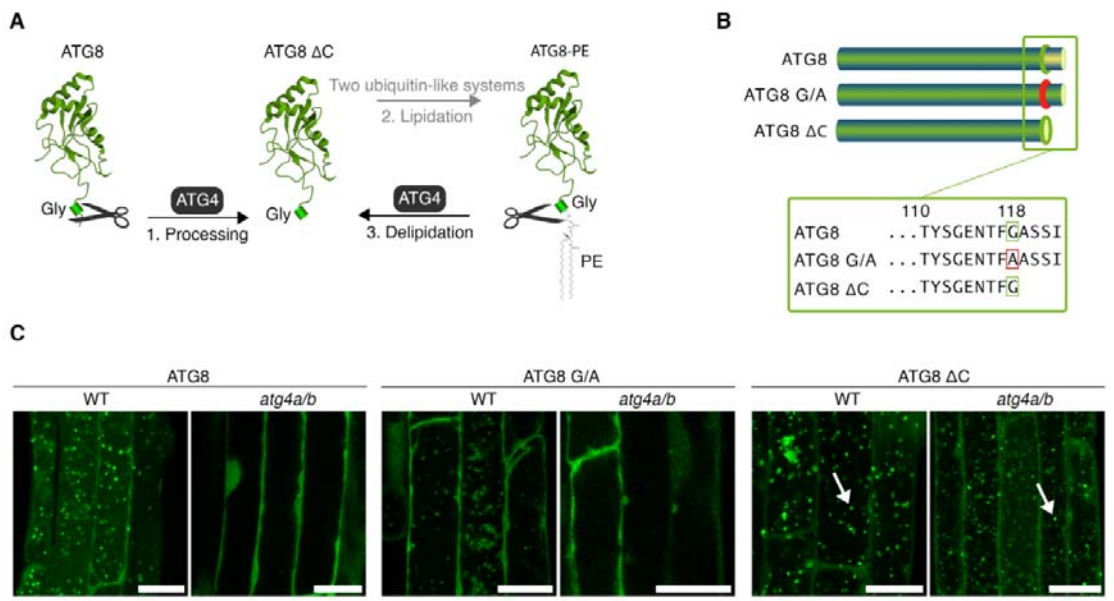

Figure 1. Essential post-translational modifications of ATG8 in Arabidopsis autophagy might not include obligatory delipidation step.

A. Schematic representation of the post-translational modifications experienced by ATG8 during autophagosome biogenesis.

B. Diagram showing C-terminal sequences of the three ATG8E variants: ATG8, full-length protein sequence including the C-terminal peptide masking the critical Gly; ATG8G/A. Full length protein in which critical Gly residue was replaced with Ala; ATG8ΔC, truncated protein lacking the C-terminal peptide that was masking the critical Gly.

C. Detection of three fluorescently labelled ATG8E variants (shown in B) in *Arabidopsis thaliana* epidermal root cells. Scale bar, 20 um.

Predictably, upon upregulation of autophagy, full length ATG8 was localizing to vacuolar puncta in the WT but remained diffuse cytoplasmic in the *atg4a/b* background. Lower intensity puncta were observed in the vacuoles of WT cells expressing G/A mutant of ATG8, indicating that it might be

taken up from the cytoplasm as a cargo. Such puncta were not observed in the vacuole of *atg4a/b* cells, corroborating lack of autophagic activity. Surprisingly, the truncated version, ATG8ΔC, was observed in the vacuolar puncta of both WT and *at4a/b*, indicating restored autophagic activity in the absence of ATG8 delipidation.

ATG8EΔC restores normal formation of autophagosome and they delivery to the vacuole in atg4a/b cells.

Next, we tested if the observed EosFP-positive puncta are indeed autophagosomes. For this we expressed the EosFP-ATG8ΔC also in the *ATG5* knockout, which is deficient in the lipidating activity and therefore would not be able to anchor EosFP-ATG8ΔC on autophagosomal membranes (**Fig 2A**).

Transgenic lines expressing truncated mutant of ATG8 were subjected to AZD/ConA treatment prior to CLSM of root and shoot epidermal cells. Indeed, upon treatment marker localized to vacuolar puncta in the WT and *atg4a/b*, but not in the *atg5* background, indicating that such localization was dependent on ATG8 lipidation (**Fig 2A**). Quantification of puncta revealed wild-type-like accumulation of autophagic bodies in the vacuoles of *atg4a/b* cells, indicating reconstituted autophagic activity in the absence of ATG8-delpidation step (**Fig.2B**).

We hypothesized that a large number of EosFP-ATG8ΔC decorated autophagosomes fusing with the vacuolar membrane would cause labelling of tonoplast (**Fig.2C**). Indeed, upregulation of autophagy, was causing accumulation of tonoplastic EoSFP signal in the *atg4a/b*, but not in the WT cells (**Fig.2D, E)**.

Next, we performed detection of the lipidated form of ATG8 by separating plant protein extract on the polyacrylamide gels containing 6 M Urea.[11,20]

Prior to protein extraction, Arabidopsis seedlings were subjected to treatment with ATG4 protease inhibitor E64-d followed by autophagy induction via AZD/ConA treatment. Consistent with the lack of ATG4 protease activity in the *atg4a/b*, we could observe the band corresponding to the ATG8-PE form in these protein extracts independently on the E64-d treatment. However, in the WT background ATG8-PE was detectable only upon E64D treatment, indicating that ATG8 delipidation occurs efficiently under normal conditions. No ATG8-PE band was detected in the protein extract of *atg5*, consistent with the lack of lipidating machinery in this mutant (**Fig.2F**).

Finally, we assessed delivery of autophagosomes to the vacuoles in the WT cells transiently lacking ATG4 activity. For this, similarly to the approach used for the **Fig.2F**, we pretreated seedlings with E64-d prior to AZD/ConA treatment (**Fig.2G**). We reasoned that constitutive cleavage of ATG8 by ATG4 should provide a large pool of ATG8 ready for lipidation, while E64-d application will terminate ATG4 activity prior to step in the autophagosome biogenesis, when ATG4 delipidates ATG8

from the surface of autophagosomes. Therefore if we still observe normal delivery of autophagosomes to the vacuoles of WT cells subjected to E64-d treatment, we will confirm dispensable role of such delipidation step for autophagy. The detected quantities of autophagic bodies in epidermal shoot and root cells were not impacted by the E64-d treatment (**Fig.2H**), thereby corroborating our observations made with genetic tools.

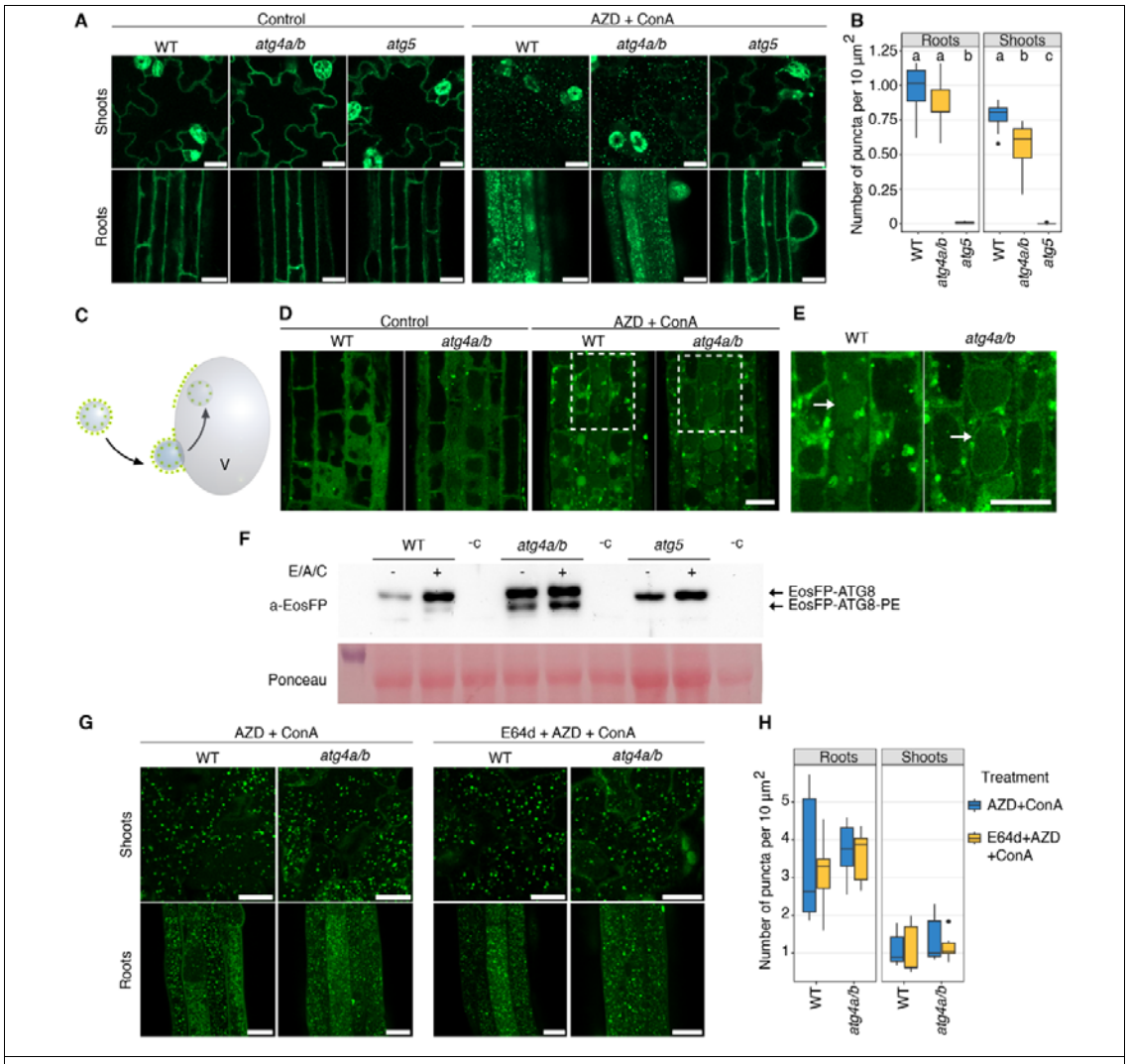

Figure 2. Delipidation of ATG8ΔE is dispensable for normal autophagosome formation.

A. Confocal microscopy images of root and shoot epidermal cells of 7 days old Arabidopsis seedlings expressing EosFP-ATG8EΔC in WT, ATG4- or ATG5-deficient backgrounds and incubated under control conditions or subjected to AZD/ConA treatment. Scale bar, 20 um.

B. Quantification of puncta per vacuolar area on the data illustrated in **A**.

C. Schematic representation of EosFP signal accumulation on the tonoplast upon its fusion with EoSP- ATG8ΔC decorated autophagosomes in the absence of ATG8-delpiation activity.

D. Confocal microscopy images of root epidermal cells expressing EosFP-ATG8ΔC and showing accumulation of tonoplastic EosFP signal in ATG4-deficeint background upon upregulation of

autophagy. Scale bar, 20 um.
E. Zoomed in images shown in **D** with adjusted contrast. Scale bar, 20 um.
F. Detection of EosFP in the protein extracts of 7 days old Arabidopsis seedlings pretreated for 8h with ATG4 inhibitor E64d prior to induction of autophagy with AZD/ConA. Ponceau staining was used as a loading control. E, E64-d; A, AZD8055; C, ConA; -c, negative control, extract of a wild-plant with no transgene.
G. Confocal microscopy images of root and shoot epidermal cells of 7 days old Arabidopsis seedlings expressing EosFP-ATG8ΔC in WT, *ATG4* knockout pretreated for 8h with ATG4 inhibitor E64d prior to induction of autophagy with AZD/ConA. Scale bar, 20 um.
H. Quantification of puncta per vacuolar area on the data illustrated in **G**.

ATG8EΔC restores wild-type like stress-tolerance in the atg4a/b.

Next, we tested if the autophagic structures observed in the *atg4a/b* background are functional autophagosomes. For this, we subjected Arabidopsis seedlings to deprivation of macronutrients (-N and -C, **Fig.3A-F**).

Seeds of WT, *atg4a/b* and *atg5* plants expressing EosFP-ATG8EΔC were plated on standard 0.5xMS growth medium, the medium depleted of nitrogen and the medium depleted of sucrose. Plates were mounted on SPIRO[21] and imaged every hour for 7 days. For -C starvation, SPIRO robots were incubated in the growth chamber without light. We observed a strong stagnation of the root growth in autophagy deficient plants (*atg4a/b* and *atg5*) deprived of macronutrients (**Fig.3A-C**). Expression of EosFP-ATG8EΔC in the WT background did not have effect on the root growth, however it reconstituted wild-type-like root growth in the *atg4a/b* background, indicating functional autophagic activity in these plants. No such effect was observed in the atg5 plants expressing EosFP-ATG8EΔC.

Additionally, we phenotyped shoots of seedlings of these transgenic lines under nitrogen and carbon depleted growth conditions (**Fig.3D-F**). In agreement with root growth assay results, expression of EosFP-ATG8EΔC decreased the negative impact of N- and C-starvation on the shoot growth of the *atg4a/b*.

Finally, we phenotyped the transgenic plants growing soil under long day conditions to detect the early senescence phenotype typical for autophagy-deficient Arabidopsis plants (**Fig.3G, H**)[22]. Consistent with the above-described phenotyping assays, we could observe alleviation of the early senescence phenotype in the *atg4a/b* plants expressing EosFP-ATG8EΔC. Therefore, we conclude that autophagic structures observed in cells of the *atg4a/b* plants upon expression of EosFP-ATG8EΔC correspond to fully functional autophagosomes.

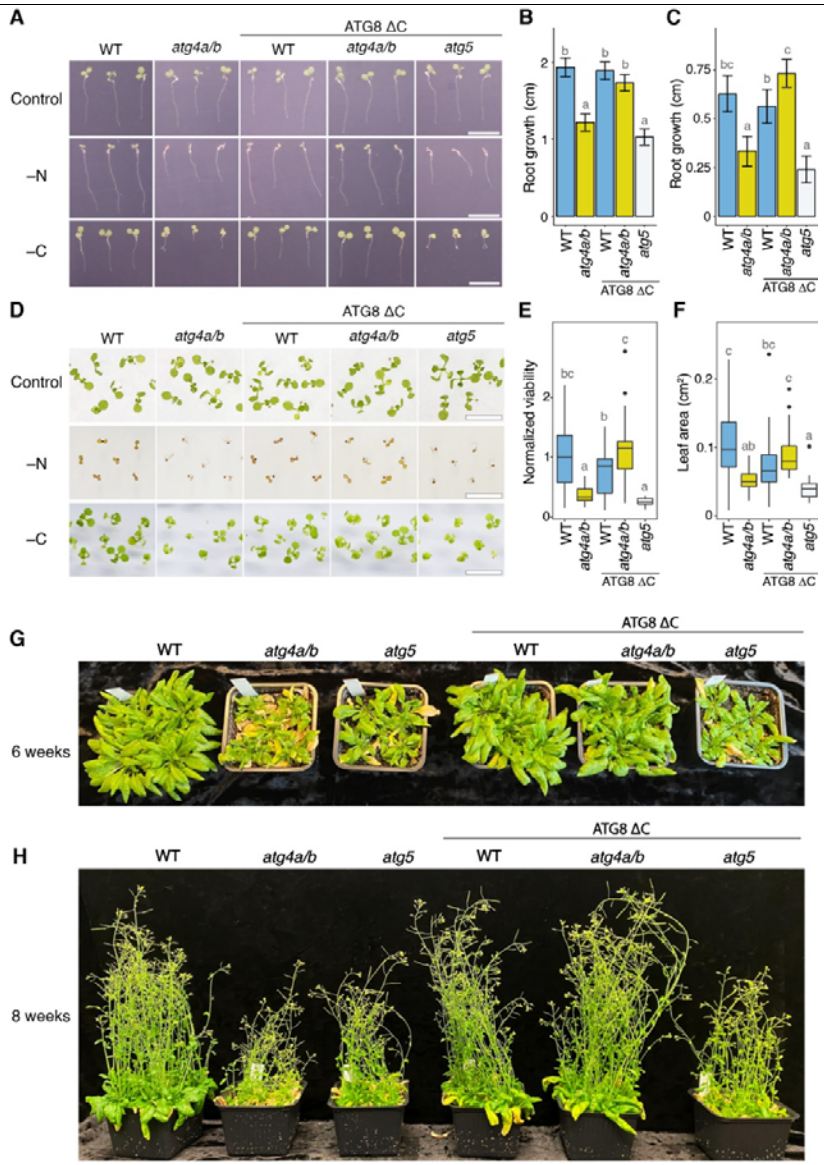

Figure 3. Expression of ATG8DE alleviates autophagy-deficient phenotypes of *atg4a/b*

A. Examples of Arabidopsis seedling roots phenotyped using SPIRO under Control, nitrogen-depleted (–N), and carbon-depleted (–C) conditions. Normal root growth under nutrient-depleted conditions is restored in *atg4a/b* seedlings expressing ATG8DC. In total, 997 biological replicates were phenotyped under –N and –C conditions in seven independent experiments.

B. Quantification of seedling root length on the 4th day after germination when grown under –N conditions, as illustrated in panel **A** (middle row). The chart represents the combined data from two independent experiments (n = 364). Root growth was analyzed by fitting a mixed-effect second-order polynomial model to the time-resolved root length data obtained by the SPIRO root growth tracking assay. Letters signify all-pairwise comparisons, where treatments sharing the same letter do not differ at the $\alpha = 0.05$ level. Error bars indicate 95% confidence interval.

C. Quantification of seedling root growth during four days of recovery following four days of carbon depletion, as illustrated in panel **A** (bottom row). The chart represents combined data from two independent experiments, n = 283. Root length was analyzed and visualized as in Panel **B**.

D. Examples of Arabidopsis seedling shoot phenotypes under Control, nitrogen-depleted (–N), and

carbon-depleted (–C) conditions.
E. Viability of Arabidopsis seedlings grown on –N medium, estimated by shoot chlorosis, as illustrated in panel D (middle row) (middle panel). Phenotyping was performed in two independent experiments. The chart summarizes data from a single experiment (n = 157). The upper and lower edges of boxes indicate upper and lower quartiles of the data, the middle line indicates the median, and the whiskers extend to data points within 1.5 * interquartile range (IQR). Dots indicate data points outside 1.5 * IQR. Treatments were compared with ANOVA and evaluated using Tukey's Honest Significant Difference test. Shared letters indicate no difference at the $\alpha = 0.05$ level.
F. Leaf areas of Arabidopsis seedling shoots at the end of a one-week-long recovery after seven days of carbon depletion, as illustrated in panel **D** (bottom row). The experiment was performed twice. Chart shows representative data from one experiment (n = 160). Results were analyzed and visualized as in Panel **E**.

Arabidopsis ATG8 isoforms differ in their capacity to restore ATG8-delipidation independent autophagic flux.

Arabidopsis genome encodes nine ATG8 orthologs, typically referred to as isoforms ATG8A-ATG8I[15]. Two of the ATG8 isoforms, ATG8H and ATG8I, do not possess the C-terminal peptide and therefore are not dependent on the processing by ATG4 for their lipidation and can be readily lipidated and used for biogenesis of autophagosomes in the *atg4a/b* mutant (**Fig.1A**, **Fig.4A**). Interestingly, ATG8I is also one of the highest expressed ATG8 genes in Arabdiopsis (**Fig.4B**). Considering our discovery that autophagy can be reestablished in the ATG4-deficeint background through the expression of truncated ATG8E, we were left to question why the naturally truncated ATG8I isoform does not similarly reinstate autophagosome formation in *atg4a/b* plants. We proposed two plausible explanations: (i) the total amount of the available to lipidation ATG8 (the sum amount of ATG8H and ATG8I) is much lower than the sum amount of all isoforms ATG8A-ATG8I available for lipidation in the WT background and might be not sufficient for normal autophagosome biogenesis; (ii) ATG8H and ATG8I isoforms play specific roles in autophagy that do not include participation in autophagosome biogenesis, e.g. sequestration of specific cargo.

To test these hypotheses, we selected two strongest expressed ATG8 isoforms, one with and one without C-terminal peptide, ATG8F and ATG8I, respectively. We generated fluorescently labelled fusions of these isoforms and expressed them transiently from a strong native Arabidopsis promoter, *APA1*, in WT, *atg4a/b* and *atg7* cells, where latter were deficient in the ATG8 lipidation activity. Upon induction of autophagy, we could observe accumulation of autophagic-body like structures in the vacuoles of WT cells expressing either of the ATG8 isoforms. Under the same conditions, vacuolar puncta were observed only in the cells of the ATG8I-expressing cells lacking ATG4. ATG8F expression in the same cells did not reconstitute autophagosome biogenesis. Expectedly, due to the absence of ATG8 lipidating activity, no puncta were observed in the vacuoles of *atg7* mutants (**Fig.4C**). These results supported out first hypothesis by showing that overexpression of ATG8I leads

to formation of autophagosomes. Additionally, we established transgenic lines expressing GFP-fusion of the same ATG8 isoforms under control of strong viral promoter. Detection of autophagic bodies in the leaves of these plants confirmed the results obtained in the transient expression system (**Fig. 4D**). Lastly, we conducted a GFP-cleavage assay on protein extracts from the plants overexpressing GFP-ATG8 isoforms. This assay measures autophagic activity based on the quantity of free GFP detected in the protein samples. Accumulation of free GFP was clearly detectable in the *atg4a/b* overexpressing GFP-ATG8I, but not GFP-ATGF (**Fig. 4E**), thus confirming autophagic activity restored by higher amount of available for lipidation ATG8. Lower efficacy of GFP-ATG8I cleavage in *atg4a/b* background in comparison to the WT also indicated that our second hypothesis might be also correct.

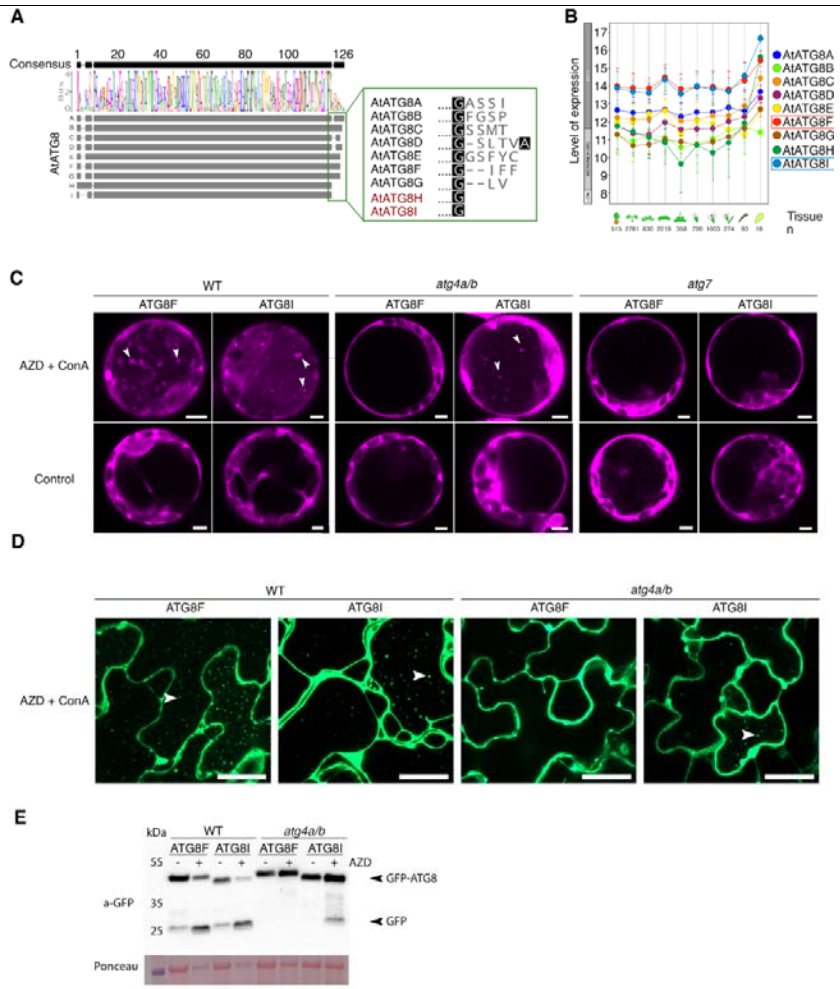

Figure 4. Overexpression of ATG8I can partially restore autophagosome formation in *atg4a/b*.

A. Schematic representation of Clustal W protein alignment of Arabidopsis ATG8 isoforms. The inset shows C-terminal sequence containing the critical for lipidation Gly residue. Notably ATG8H and ATG8I do not possess C-terminal peptide and have the critical Gly readily exposed.

B. GENEVESTIGATOR data on organ-specific expression of all nine ATG8 isoforms of Arabidopsis. ATG8F (bright red) rectangle and ATG8I (light blue) isoforms are the best expressed

isoforms.
C. Detection of autophagic bodies in the vacuoles of protoplast obtained from WT, *atg4a/b* and *atg7* (deficient in ATG8 lipidating activity) mutants transformed with TagRFP-labelled ATG8F or ATG8I. Scale bar, 5 um.
D. Detection of autophagic bodies in the vacuoles of stable transgenic lines expressing GFP-tagged ATG8F or ATG8I in WT or *atg4a/b*. Leaves were infiltrated with AZD/ConA 24h prior to imaging. White arrowheads point at autophagic bodies. Scale bar, 25 um.
E. GFP-cleavage assay performed on the transgenic lines illustrated in **D**, shows restored accumulation of free GFP in the *atg4a/b* plants expressing GFP-ATG8I. Autophagy was induced by infiltrating leaves with AZD 24h prior to sampling.

Autophagy independent from ATG8 delipidation is not conserved in the green algae lineage.

To investigate whether delipidation of ATG8 is dispensable for autophagy in other lineages, we conducted experiments on the unicellular green alga, *Chlamydomonas reinhardtii*, a close relative of plants. We generated *cratg4*, *cratg5*, *cratg7*, and *cratg8* autophagy-deficient mutants in the UVM4 background (**Fig.5A**) and complemented them with mCherry-tagged CrATG8 or CrATG8ΔC. Immunoblot analysis of the established transgenic lines confirmed a good expression level of the mCherry-CrATG8s in *cratg4*, *cratg5*, *cratg7* backgrounds and variable but detectable expression in the *cratg8* background (**Fig.5B**). These lines were subjected to a growth assay after being cultured in TAP medium for 40 days. Interestingly, expression of the truncated form of ATG8 did not rescue the poor growth rate of the *cratg4* mutant (**Fig.5B**). Similarly, *cratg5* and *cratg7* mutants, which lack the intact pathway of autophagosome formation, exhibited growth defects (**Fig.5B**). In contrast, the *cratg8* knockout complemented with CrATG8 or CrATG8ΔC, demonstrated a direct correlation between the transgene expression and growth rate (**Fig.5B**). The strain with high expression of CrATG8ΔC displayed a growth phenotype similar to that of the wild-type line. Taken together, our data suggest that the ATG8 delipidation process is essential for growth in *Chlamydomonas reinhardtii*.

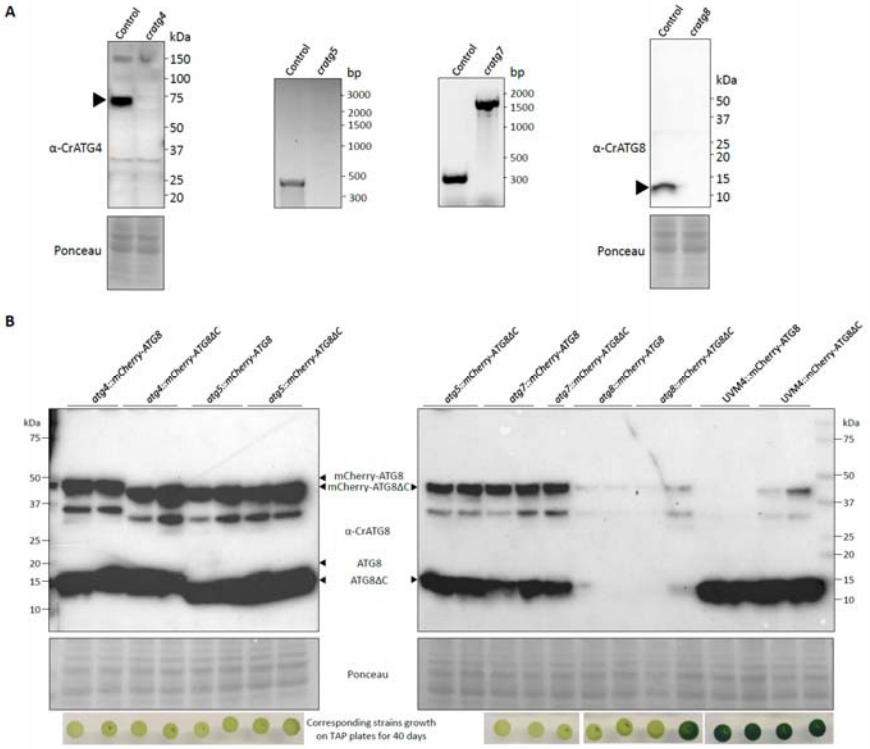

Figure 5. Delipidation of ATG8 is critical for autophagy in *Chlamydomonas reinhardtii*.

A. Validation of generated Chlamydomonas knockout mutants lacking ATG4, ATG5, ATG7 or ATG8 by Western blot (CrATG4 and CrATG8) or genotyping (CrATG5 and CrATG7).

B. Western blot detection of endogenous ATG8 and mCherry-ATG8 transgene expression in the established lines. Ponceau staining was used as a loading control. The bottom panel demonstrates the phenotype of corresponding line grown on the TAP medium for 40 days. Light color of cell colonies indicates poor nutrient deficiency tolerance in the corresponding line caused by dysfunctional autophagy.

Discussion

Autophagy was likely invented by the Last Eukaryotic Common Ancestor (LECA)[23] to maintain the newly acquired complex cell structures, such as organelles. During eukaryotic evolution, autophagy has diversified to adapt to various life strategies (autotrophic *vs*. heterotrophic), mobility traits (sessile *vs*. mobile), forms of life (unicellular *vs*. multicellular), nutrient requirements, and specific configurations of endomembrane trafficking systems observed in fungi, animals, and plants. For example, eukaryotes evolved different configurations of the lytic compartment - the final destination of the autophagic pathway. The main lytic compartment of animal cells are lysosomes: compact and mobile organelles. The modest size of lysosomes and their importance for other cellular pathways, compels animal cells to regeneratee these organelles after their fusion with autophagosomes in a process known as autolysosome recovery (ALR)[24]. Such process has not been yet reported for fungal and plant cells, in which autophagosomes fuse with the large lytic vacuoles that often occupy most of the cell volume[1,2].

Notably, autophagosome biogenesis in yeast cells occurs in proximity of the vacuole, at the single phagophore assembly site (PAS). Consequently, once complete, autophagosomes fuse immediately with vacuoles. In contrast, autophagosomes in animal cells emerge at multiple locations, and are trafficked towards nuclei to fuse there with the perinuclearly translocated lysosomes[25]. Interestingly, plants' autophagic strategy seems to be somewhere in-between the yeast and animal solutions. That is, autophagosomes form at multiple foci and are trafficked towards the immobile large lytic vacuole[2]. In view of these facts, it is conceivable that despite conservation of the core autophagic mechanisms, some molecular aspects of the pathway might significantly differ in plants, fungi and animal cells.

Based on our observations, we propose that plant autophagosome maturation diversified into strategies dependent and independent from ATG4 delipidating activity. Further studies are required to determine the molecular components governing these two strategies. Additionally, we demonstrate that ATG8 isoforms of Arabidopsis can contribute to a different extent to autophagosome biogenesis. This is a new insight on the potential reason behind expansion of the ATG8 gene family in plants.

Competing interests

The authors declare no competing interests.

References

1. Mizushima, N. A brief history of autophagy from cell biology to physiology and disease. *Nat Cell Biol* **20**, 521–527 (2018).

2. Marshall, R. S. & Vierstra, R. D. Autophagy: The Master of Bulk and Selective Recycling. *Annu Rev Plant Biol* **69**, 173–208 (2018).

3. Zhang, S., Hama, Y. & Mizushima, N. The evolution of autophagy proteins – Diversification in eukaryotes and potential ancestors in prokaryotes. *Journal of Cell Science* vol. 134 Preprint at https://doi.org/10.1242/jcs.233742 (2021).

4. Martens, S. & Fracchiolla, D. Activation and targeting of ATG8 protein lipidation. *Cell Discovery* vol. 6 Preprint at https://doi.org/10.1038/s41421-020-0155-1 (2020).

5. Ichimura, Y. *et al.* A ubiquitin-like system mediates protein lipidation. *Nature* **408**, 488–492 (2000).

6. van der Veen, A. G. & Ploegh, H. L. Ubiquitin-Like Proteins. *Annu Rev Biochem* **81**, 323–357 (2012).

7. Romanov, J. *et al.* Mechanism and functions of membrane binding by the Atg5-Atg12/Atg16 complex during autophagosome formation. *EMBO Journal* **31**, (2012).

8. Martens, S. & Fracchiolla, D. Activation and targeting of ATG8 protein lipidation. *Cell Discovery* vol. 6 Preprint at https://doi.org/10.1038/s41421-020-0155-1 (2020).

9. Kirisako, T. *et al.* The reversible modification regulates the membrane-binding state of Apg8/Aut7 essential for autophagy and the cytoplasm to vacuole targeting pathway. *Journal of Cell Biology* **151**, 263–275 (2000).

10. Abreu, S. *et al.* Conserved Atg8 recognition sites mediate Atg4 association with autophagosomal membranes and Atg8 deconjugation. *EMBO Rep* e201643146–e201643146 (2017) doi:10.15252/embr.201643146.

11. Yoshimoto, K. Processing of ATG8s, Ubiquitin-Like Proteins, and Their Deconjugation by ATG4s Are Essential for Plant Autophagy. *the Plant Cell Online* **16**, 2967–2983 (2004).

12. Nair, U. *et al.* A role for Atg8-PE deconjugation in autophagosome biogenesis. *Autophagy* **8**, (2012).

13. Nakatogawa, H., Ishii, J., Asai, E. & Ohsumi, Y. Atg4 recycles inappropriately lipidated Atg8 to promote autophagosome biogenesis. *Autophagy* **8**, 177–186 (2012).

14. Kellner, R. *et al.* ATG8 Expansion: A Driver of Selective Autophagy Diversi fi cation? *Trends Plant Sci* **22**, 204–214 (2017).

15. Kellner, R. *et al.* ATG8 Expansion: A Driver of Selective Autophagy Diversi fi cation? *Trends Plant Sci* **22**, 204–214 (2017).

16. Zess, E. K. *et al.* N-terminal β-strand underpins biochemical specialization of an ATG8 isoform. *PLoS Biol* **17**, (2019).

17. Kauffman, K. J. *et al.* Delipidation of mammalian Atg8-family proteins by each of the four ATG4 proteases. *Autophagy* **14**, (2018).

18. Yu, Z.-Q. *et al.* Dual roles of Atg8-PE deconjugation by Atg4 in autophagy. *Autophagy* **8**, 883–892 (2012).

19. Dauphinee, A. N. *et al.* Chemical screening pipeline for identification of specific plant autophagy modulators. *Plant Physiol* **181**, 855–866 (2019).

20. Chung, T., Phillips, A. R. & Vierstra, R. D. ATG8 lipidation and ATG8-mediated autophagy in Arabidopsis require ATG12 expressed from the differentially controlled ATG12A and ATG12B loci. *Plant Journal* **62**, 483–493 (2010).

21. Ohlsson, J. A. *et al.* SPIRO-the automated Petri plate imaging platform designed by biologists, for biologists. *bioRxiv* 2021.03.15.435343-2021.03.15.435343 (2021).

22. Yoshimoto, K. *et al.* Autophagy Negatively Regulates Cell Death by Controlling NPR1-Dependent Salicylic Acid Signaling during Senescence and the Innate Immune Response in Arabidopsis. *THE PLANT CELL ONLINE* **21**, 2914–2927 (2009).

23. Koumandou, V. L. *et al.* Molecular paleontology and complexity in the last eukaryotic common ancestor. *Critical Reviews in Biochemistry and Molecular Biology* vol. 48 Preprint at https://doi.org/10.3109/10409238.2013.821444 (2013).

24. Chen, Y. & Yu, L. Development of research into autophagic lysosome reformation. *Molecules and Cells* vol. 41 Preprint at https://doi.org/10.14348/molcells.2018.2265 (2018).

25. Yim, W. W. Y. & Mizushima, N. Lysosome biology in autophagy. *Cell Discov* **6**, (2020).